



Published in final edited form as:

Anal Chem. 2010 March 15; 82(6): 2192–2203. doi:10.1021/ac9024889.

Single-Molecule Spectroscopy and Imaging of Biomolecules in Living Cells

Samuel J. Lord, Hsiao-lu D. Lee, and W. E. Moerner

Department of Chemistry, Stanford University, Stanford, California 94305-5080

The number of reports per year on single-molecule imaging experiments has grown roughly exponentially since the first successful efforts to optically detect a single molecule were completed over two decades ago. Single-molecule spectroscopy has developed into a field that includes a wealth of experiments at room temperature and inside living cells. The fast growth of single-molecule biophysics has resulted from its benefits in probing heterogeneous populations, one molecule at a time, as well as from advances in microscopes and detectors. This Perspective summarizes the field of live-cell imaging of single biomolecules.

Introduction

Single-molecule biophysics spans a range of experiments, from force studies of single macromolecules using tweezers¹⁻³ or cantilevers⁴ to in vitro assays of fluorogenic enzymatic turnovers.⁵ For instance, by decorating a biomolecule with many copies of a probe, researchers have studied single DNA strands,^{6, 7} membrane molecules,⁸ motors,⁹ and viruses.¹⁰ In this Perspective, we focus instead on single-molecule spectroscopy and imaging (SMS) experiments, which measure the signal from one individual fluorescent label in a living cell. Moreover, in the interest of space, we will not discuss the related area of fluorescence-correlation spectroscopy,¹¹ although the method can probe the ensemble dynamics of single emitters and has been applied to living cells.¹²

The main reason for performing SMS is the ability to measure the full distribution of behavior instead of a single population average, thus exposing normally hidden heterogeneities in complex systems. A full distribution of an experimental parameter provides more information than the ensemble average; for instance, the shape of the distribution may be skewed or reveal multiple subpopulations, which may offer insight into underlying mechanisms. Each single molecule is a local reporter on the makeup and conditions of its immediate surroundings—its “nanoenvironment”—and thus acts as a readout of spatial heterogeneity of a sample. SMS also measures time-dependent processes that are not necessarily synchronized throughout the sample or population. For example, multiple catalytic states of an enzyme will be convolved with all the states of other copies in an ensemble, whereas a SMS experiment can measure uncorrelated stochastic transitions of a single enzyme. SMS also has the ability to observe intermediate states or rare events, given that the instruments have sufficient time resolution.

Because living systems are highly complex samples, with spatial and temporal heterogeneities that have biological relevance and with a wealth of processes that operate at the single-biomolecule level, SMS is a powerful tool to better understand the processes involved in life. Without needing to synchronize populations of biomolecules or cells, SMS is able to record the time evolution of these samples, for instance showing the sequence of events in a pathway. In many situations, fluctuations and rare events may be essential to biological function, making

studying each single molecule that much more powerful. Finally, sparsely labeling a population of biomolecules (as is sufficient for many SMS experiments) reduces the chances that the probe will interfere with the biology one is studying. For these reasons, SMS is quickly becoming a popular technique in biophysics and cell biology.

History of SMS and Biophysics

The optical absorption of single molecules was originally detected in solids at cryogenic temperatures by direct sensing of the absorbed light;¹³ subsequently, researchers detected optical absorption by measuring the fluorescence from single emitters under similar conditions.¹⁴ In the early experiments, optical saturation, spectral diffusion, photon antibunching, resonant Raman, electric field effects, and magnetic resonances of single molecules were observed.¹⁵ Optical detection of single molecules was eventually performed at room temperature from burst analysis in solution,¹⁶⁻¹⁸ in microdroplets,¹⁹ using near-field tips,²⁰ and by 3D nanoscale tracking of single emitters in porous gels.²¹

As single-molecule techniques addressed biologically relevant systems and samples at room temperature, biophysics quickly became an active target of SMS research.^{15, 22, 23} Single copies of fluorescent proteins (FPs) were imaged and the ability to control photoswitching was demonstrated,²⁴ Förster-resonance-energy transfer (FRET) was observed on the single-pair level,²⁵ the diffusion of single emitters was recorded in a phospholipid membrane,²⁶ single motor proteins were imaged,²⁷⁻²⁹ and the nucleotide-dependent orientations of single kinesin motors were measured.³⁰

Studying living cells can be significantly more difficult than *in vitro* samples or fixed cells, because a living cell is a complex environment with elaborate interactions among components and cells exhibit continually changing states. Nevertheless, the reasons that make living cells tricky to study are fundamental characteristics of biology, and better understanding these attributes is critical to a deeper understanding of actual biological processes. See Table 1 for a selected timeline of SMS experiments with relevance to living cells.

Basic Requirements for SMS in Living Cells

SMS traditionally requires a transparent, nonfluorescent host matrix; molecules that are resolved by separating them in space (by more than the diffraction limit of ~200 nm), time, or wavelength; and probes that are efficient absorbers, highly fluorescent, and exceptionally photostable.

Imaging single emitters in living cells introduces further challenges. (1) In order to maintain low background counts, one must avoid cellular autofluorescence, the result of exciting endogenous cellular fluorophores (e.g. flavins, NADH, tryptophan). Autofluorescence can be avoided by selecting an imaging wavelength longer than about 500 nm, where biological fluorophores typically do not absorb, and by using cell growth media and imaging buffers that are free of fluorophores. (2) The cell membrane is a significant barrier to cell entry, because the probe must be able to pass through the hydrophobic lipid bilayer. Choosing a genetically expressed or membrane-permeable probe is critical for intracellular labeling, unless microinjection or electroporation is performed. (3) One of the primary challenges to live-cell imaging is specific labeling of predetermined sites on proteins or oligonucleotides. Due to the complex chemical environment inside cells, many bioconjugation reactions used *in vitro* (e.g. maleimide with cysteine or N-hydroxysuccinimide ester with lysine) are not sufficiently selective. Therefore, bioorthogonal labeling reactions are necessary for targeting organic fluorophores to biomolecules of interest in the cell.^{31, 32} More commonly, researchers have relied on the genetic expression of FPs for single-molecule biophysics in living cells. (4) After an exogenous probe is targeted inside the cell, the difficulty of washing out unbound copies

introduces further complications. Therefore, there must be a method to reject spurious signal from non-targeted fluorophores. For instance, this can be accomplished by employing fluorogenic labeling reactions^{33, 34} or by adjusting the detector integration times to average out the signal (spread over many pixels) from quickly diffusing unbound fluorophores.^{35, 36} (5) Finally, it is imperative that the experiment does not significantly interfere with the relevant biology of the cell. High labeling ratios, large probe size, photoradical production, and genetic manipulation can change phenotypes or even kill cells. Thus, careful controls are necessary to ensure that the labeling technique, sample preparation, and imaging conditions do not alter the physiology of interest.

Probes and Labeling

Probes

As FPs are powerful tools used extensively in biological imaging,^{37, 38} it is not surprising that they are also important for live-cell SMS.^{39, 40} To minimize background, longer-wavelength FPs (e.g. EYFP and other orange- or red-emitting FPs) are most desirable; therefore, there has been a sustained effort to tune FPs to longer wavelengths and to impart other beneficial qualities (e.g. photostability, brightness, monomeric or tandem dimers).⁴¹

The major drawback to FPs is that they are generally an order of magnitude less photostable than many small organic fluorophores, which can emit millions of photons before photobleaching.^{42, 43} Commonly used classes of organic fluorophores include the following: Cy3 and other carbocyanine dyes, rhodamines,⁴⁴ fluoresceins,⁴³ DCDHFs,³⁴ terrylene and rylens,⁴⁵ etc.

Quantum dots (QDs) are semiconductor nanocrystals that photophysically act like fluorescent molecules for most purposes.^{46, 47} Other nanoparticles are also used in imaging, such as scattering centers and nanoclusters.^{48, 49} While QDs and nanoparticles are typically very photostable, they are much larger than organic fluorophores or FPs, their emission blinks in a complex way, and their large size may hinder motion of the analyte and obfuscate the true dynamics. However, this problem is mitigated by the fact that, at the low Reynolds numbers that these particles experience, drag forces are linear with velocity and radius (instead of scaling with the square of both, as they would at the high Reynolds numbers of everyday human experience). Unfortunately, QDs and nanoparticles are usually endocytosed and remain trapped in endosomes instead of entering the cytosol, so they have faced hurdles in targeting in live cells.

Finally, several groups have developed photoswitchable or photoactivatable probes, which are necessary for super-resolution microscopies, pulse-chase imaging, photoactivation-tracking experiments and more: FPs,^{24, 50, 51} Cy3-Cy5 pairs,⁵²⁻⁵⁴ DCDHFs,⁵⁵ rhodamines,⁵⁶ merocyanines,⁵⁷ QDs,⁵⁸ nanoparticles,⁵⁹ and others.⁶⁰ See Table 2 for more information about fluorescent probes used in live-cell SMS.

Labeling

There are several labeling strategies for live-cell imaging (see Table 3). Genetic expression of FPs directly provides specific labeling, and thus most live-cell SMS experiments have imaged FPs fused to proteins of interest. Targeting exogenous probes such as organic fluorophores or nanoparticles poses a significant challenge, but offers the benefits of more photostable or photochemically sophisticated fluorophores, as well as possible reduction in size and steric effects.

Strong but noncovalent binding to short peptide motifs has been demonstrated by Tsien and others using FIAsh-type fluorophores.³³ Although ReAsH has been imaged on the single-

molecule level in vitro,⁶¹ live-cell SMS imaging with FAsH-type fluorophores have faced problems of off-target labeling and low photostability.³⁷

Irreversible bioconjugation of fluorophores with pendant chemical “tags” to engineered enzymes genetically fused to proteins of interest has the potential to compete with FP labeling.^{32, 62} For instance, SNAP-tags and HaloTags are two such fusion enzymes, which react with synthetic benzylguanine and chloroalkane tags, respectively; after the reaction, the tag—and any probe linked to the tag—are covalently linked to the enzyme, and thus to the protein of interest. In another enzymatic strategy, Sfp-labeling uses a CoA-modified fluorophore and a peptide tag on the protein of interest, which are covalently coupled by an extrinsic enzyme.

Instrumentation

The instruments and methods used for SMS have been extensively described and reviewed elsewhere;⁶³ here, we summarize a few of the basic techniques.

Microscope Configurations

SMS experiments generally use inverted optical fluorescence microscopes, configured in either wide-field illumination or confocal (see Figure 1). The simplest wide-field method is epifluorescence, in which an expanded excitation beam is focused at the back focal plane of the objective, producing a collimated illumination beam at the sample. Fluorescence is collected through the same objective, filtered from any scattered excitation light using a dichroic mirror and long-pass or bandpass filters, and imaged onto a camera.

Because epifluorescence excites a large volume of sample, background signal from out-of-focus emitters can interfere in imaging thick samples. Total-internal-reflection fluorescence (TIRF) imaging solves this problem by exciting only a thin slice of the sample nearest the coverslip. Excitation light is directed into the objective off center, causing the beam to totally internally reflect at the coverslip, subsequently producing a quickly decaying evanescent field up from the surface. The fluorescence excited by the evanescent field is collected through the objective, filtered, and imaged using a camera. Because the evanescent field falls off exponentially within ~100 nm, TIRF is useful when the region of interest is very near the coverslip. A variation called quasi-TIRF (also referred to as “pseudo-” or “leaky-TIRF”) also sends in the excitation beam off-center, but not far enough for total-internal reflection; instead, a highly angled beam exits the objective and illuminates the sample in a slice thicker than TIRF but thinner than epifluorescence.

Another method to reduce out-of-focus fluorescence is confocal microscopy, which is a point-detection, scanning technique. A collimated excitation beam that slightly overfills the back aperture of the objective is directed into the microscope, producing a diffraction-limited spot at the sample. The confocal spot is scanned across the sample and emission is collected through the objective, filtered, focused through a pinhole (which rejects out-of-focus light), recollimated, then focused onto a point detector. Confocal imaging is not constrained to be near the coverslip, so can be used to image deeper into a sample or for three-dimensional scanning. The primary drawback of confocal is that it requires scanning the stage or the beam and a point detector, so multiple parts of the sample cannot be imaged simultaneously. This makes widefield configurations much more practical for single-particle tracking and imaging dynamic structures.

Detectors

In order to measure the stream of photons from a single emitter, a detector must exhibit low dark counts, high quantum efficiencies over a range of wavelengths, and low noise (from readout, electron multiplication, or analog-to-digital conversion). For details regarding detector

types, characteristics and capabilities of different detectors, quantitative resolution and sensitivity parameters, sufficient signal-to-noise ratios for SMS detection, and other technical details see references^{63, 64}.

There are two classes of detectors for SMS, single-element or point detectors, and two-dimensional array detectors. Point detectors for confocal imaging include photomultiplier tubes (PMT), avalanche photodiodes (APD or SPAD), or hybrids thereof. While PMTs have large detection area ($\sim 1 \text{ cm}^2$) and ps–ns time resolution, APDs have higher quantum efficiencies and more easily detect single photons; moreover, APDs have very low dark counts, have faster time resolution, and output a digital signal that can easily be interfaced with a computer. The major drawbacks of APDs are (a) the small detection area, which makes aligning onto the sensor more difficult, and (b) the limited photon detection rates.

Wide-field imaging configurations allow the use of multidetector arrays or cameras, such as charge-coupled devices (CCD). Modern Si CCDs often include on-chip electron multiplication to increase sensitivity and reduce readout noise; moreover, frame-transfer technology permits faster imaging rates by performing the slow readout step on a separate, dark section of the chip. These cameras typically have quantum efficiencies $>80\%$ for the visible spectrum and frame-integration times of 10–100 ms, or faster for fewer pixels.

Optics

High quality lenses, mirrors, and filters are especially important for the ultrasensitive detection required for SMS. Immersion objectives with high numerical aperture (NA ~ 1.4) are necessary to collect as much of the emission as possible, but can complicate polarization. In addition, objectives for SMS should be achromatic and corrected for the coverslip material and thickness. Objectives specifically designed for TIRF are carefully designed to allow the excitation beam to be far off center.

Optical filters and dichroic mirrors must not fluoresce, must pass as much fluorescence as possible, and must reject all pump scattering and as much spurious signal as possible. Thus, long-pass filters must have sharp cut-on spectra, with optical density 6+ at shorter wavelengths. Bandpass filters can be helpful to remove longer-wavelength background fluorescence or excess Raman scattering from water, but it is important to overlay the filter's transmission spectrum with the emission spectrum of the fluorescent label to avoid rejecting too much of the emission. Filters and lenses inside the microscope should be anti-reflection coated and aberration-corrected. For instance, thin dichroics can easily bend and distort the image; 2-mm or thicker dichroics are preferable.

Sources

Light sources for SMS are many, but are usually lasers. Single-frequency dye lasers were used in the early cryogenic SMS experiments, where finding the narrow absorbance peaks required tuning the excitation light. At room temperature, gas (e.g. argon-ion, helium-neon, etc.), diode, or solid-state lasers are typically used. While lasers are necessary for some techniques, epifluorescence excitation is possible using broadband sources such as arc lamps or light-emitting diodes. White-light or fiber lasers can also provide broadband light, produced by nonlinear optical effects when high-energy pulses (from a titanium-sapphire or other pulsed laser) are transmitted through special optical fibers. Broadband sources can be convenient because they are tunable to a range of colors, but are more difficult to filter than a monochromatic excitation source. In all cases, the excitation source should be filtered to reject unwanted leakage of the other colors or laser lines.

SMS Imaging in Living Cells

Early work imaging single molecules in living cells has been reviewed elsewhere.^{23, 65, 66} We will briefly touch on these earlier studies, which primarily involved tracking single proteins in cell membranes, but also summarize a wide range of more recent experiments (see Table 1 and Figure 2).

Molecules in Membranes

Fast CCD cameras have made it possible to image in widefield and track in real time single molecules moving in plasma membranes.^{67, 68} The membrane of living cells was an early target of SMS, especially in attempts to observe the elusive lipid “rafts” or other structures and domains: by tracking single proteins or emitters, researchers probed tiny regions to search for heterogeneous dynamics. Kusumi et al.⁶⁹ applied high-speed particle tracking, with frame rates as high as 40 kHz, to observe the movements and confinement of molecules in the plasma membrane. Hop diffusion between submicron regions was observed, hinting of a “picket fence” model of membrane rafts (i.e. that bulky transmembrane proteins are corralled by the membrane-associated cytoskeletal filaments).⁷⁰

A team led by Moerner and McConnell tracked fluorescently labeled transmembrane proteins and measured the large decrease in diffusion by depleting cholesterol (see Figure 3).^{71, 72} They also measured the diffusion dynamics of single small, lipid-like fluorophores embedded in the lipid bilayer.⁷³ Originally, these studies indicated that the diffusion of the transmembrane protein called the major histocompatibility complex of type II and its glycolipid-anchored form was not altered after actin was depolymerized. Because actin provides the cytoskeletal structure, these results seemed to contradict the picket fence model. A more recent re-examination of the same system at higher time resolution by both groups revealed some evidence of membrane compartments.⁷⁴ Nevertheless, the existence of lipid rafts in living cells is still contentious in the membrane community, and more studies will be necessary before any models are widely accepted.

Many biomedical researchers seek small proteins that assist cargo to enter cells, often drugs or genetic material that otherwise could not pass the plasma membrane. Lee et al.⁷⁵ tracked single DCDHF-labeled polyarginines to determine possible entry mechanisms for cell-penetrating peptides (see Figure 3). Quantitative analyses of the peptides interacting with the plasma membrane indicated that polyarginines enter the cell via multiple pathways or via a mechanism other than passive diffusion or endocytosis, which may have implications in the biomedical uses of arginine-based cell-penetrating peptides and their cargo.

Longer tracking times require emitters that are photostable for minutes, such as QDs or nanoparticles. Dahan et al.⁷⁶ labeled glycine receptors in the membranes of living neurons, tracked for minutes and observed multiple domains of the cell surface, as single receptors diffused from synaptic regions to areas outside the synaptic membrane. They also recorded cell-entry events, confirmed later using electron microscopy. Given that QDs are large, the authors expressed concern that the size of the probe might have hindered motion of the receptors in the synapse; while such hindrance could not be fully ruled out, a comparison with a relatively small antibody labeled with the organic fluorophore Cy5 revealed equal percentage of rapidly diffusion receptors with either label. Besides these concerns with the large size, the QD labels permitted long imaging times and their brightness resulted in higher-precision tracking.

Transmembrane ion channels are also an interesting target for SMS high-precision tracking. Harms et al.⁷⁷ imaged ion channels labeled with FPs in live cells, measuring lateral diffusion, polarization, and stoichiometry of single proteins and aggregates. Schütz et al.⁷⁸ localized in three dimensions single Cy5-labeled hongotoxin molecules, which bind with high affinity to

potassium channels. These studies accessed information about the lateral, rotational, and axial motion of ion channels and associated toxins; they primarily served as proof-of-principle experiments, demonstrating the power of single-molecule tracking in multiple dimensions and with high precision.

There are numerous other proteins, structures, and processes in the plasma membrane that warrant further research. Ueda et al.⁷⁹ studied how cells detect and move in chemical gradients: by labeling cyclic adenosine monophosphate (cAMP) with Cy3, they observed its binding kinetics to chemotactic receptors in different regions of the membrane of live *Dictyostelium discoideum* cells. For instance, the dissociation kinetics of cAMP were significantly altered in a mutant cell line lacking G protein, a molecular switch coupled to the receptor and involved in the chemotaxis signaling pathway. Other researchers have applied SMS to count the number of subunits in membrane-bound proteins by counting the number of photobleaching steps,^{80, 81} which is important for better understanding of protein-protein interactions and subunit assembly.

Molecules in the Nucleus

In eukaryotic cells, biology that occurs inside the nucleus is essential to cell processes. Nuclear pores are large protein complexes that form selective holes in the nuclear envelope, the double lipid bilayer that forms the nucleus. Nuclear pores allow the transport of RNA and proteins involved in gene replication between the cytoplasm and the nucleus. Given the essential role of the nuclear pore, understanding how single biomolecules interact with the complex would be valuable. Yang et al.⁸² imaged nuclear pore complexes in living HeLa cells, recording the trajectory of single copies of substrates (labeled with one or two Alexa-555 fluorophores) undergoing transport through the pores. They were able to construct a high-resolution map of the pores from such traces (see Figure 3). Other researchers have performed more in-depth studies of the dwell times of single molecules interacting with nuclear pore complexes.⁸³

Because the nuclear envelope is an efficient barrier, introducing exogenous molecules into the nucleus can be challenging. In order to get around this problem, Knemeyer et al.⁸⁴ microinjected directly into the nucleus fluorescent oligonucleotides, which hybridized with mRNA strands. The researchers then used a pulsed laser source and fluorescence-lifetime confocal imaging to separate the relevant signal from the autofluorescence background, which exhibited a shorter lifetime. Apparent blinks in the signal from a few spots offered some evidence that the researchers were indeed imaging single fluorophores. Although primarily a proof-of-principle study demonstrating the feasibility of both microinjection and lifetime-separated fluorescence imaging, it opens the doors for subsequent experiments to examine more complicated biology that occurs within the nucleus.

Cytoskeletal Molecules

Because of their small size and the relative lack of understanding of their structural components, prokaryotes are especially interesting for single-molecule imaging. A team led by Moerner, Shapiro, and McAdams has studied protein localization and movement in living cells of the bacteria *Caulobacter crescentus* using FP fusions as fluorescent labels.^{35, 85-87} In a high-precision tracking study, they observed the movement of MreB proteins (an actin homolog).³⁵ Protein motion was measured at two different time scales: the diffusion of free monomers of MreB was recorded with CCD integration times of 15 ms yielding diffusion coefficients on the order of $1 \mu\text{m}^2 \text{s}^{-1}$; using time-lapse imaging, the speed of the slower, directed “treadmilling” motion of labeled copies incorporated into the MreB filament was measured at approximately 6 nm s^{-1} . (Treadmilling occurs when monomers add to one end of the filament while the other end dissociates, resulting in a labeled segment moving through the relatively stationary filament.) Because this treadmilling motion was so slow, single fluorophores are

likely to photobleach before a long enough trace it acquired. Instead, the motion was measured with time-lapse, using 100-ms integration times separated by up to 10 s of darkness. At these longer frame-integration times, signal from diffusing monomers was spread over many pixels, thus was only recorded as background; light from a slowly moving copy in the filament was concentrated on a few pixels and appeared as signal above the background as a diffraction-limited spot. Tracing out these slowly moving spots revealed super-resolution maps of MreB filaments (see Figure 4).

In a separate study, the same team visualized single copies of FP-labeled PopZ, a protein that anchors the chromosome origins, and its excursions between poles of *C. crescentus* cells.⁸⁶ Most copies of the protein diffused throughout the cell, while some stopped moving after reaching a cell pole. Such dynamics corroborate a diffusion-and-capture model for PopZ localization at cell poles.

Other researchers have also used live-cell SMS to study protein localization in bacteria. Niu et al.⁸⁸ photoactivated FPs and tracked single monomers of the cytoskeletal protein FtsZ, a homolog of tubulin, and imaged helical patterns of the polymerized form in *Escherichia coli* cells. They also found that monomeric FtsZ molecules moved throughout the entire cell and consistently exhibited anomalously slow diffusion at long time scales, suggesting that the monomers encounter barriers in the membrane or in the cell. These studies expanded the limited knowledge about bacteria structural and chromosomal organization, as well as explored the mechanisms of cell division.

Trafficking of Single Molecules inside Cells

Understanding how signaling molecules, cellular components, and viruses are trafficked in living cells is an important goal in biomedical imaging. A team led by Chu and Mobley labeled nerve growth factor (NGF) with single QDs and tracked their transport in the axons of living neurons, concluding that a single NGF is sufficient to initiate signaling.⁸⁹ By observing individual endosomes being trafficked along the axon toward the cell body, they were able to record a variety of behaviors, such as stop-and-go, short retrograde movement, and multiple endosomes pausing at the same location in an axon. Moreover, labeling with only a single QD offered information that would have been obscured with many labels: a majority of the endosomes contained only one single NGF–QD conjugate. This claim was made after observing a photoblinking signal, which is indicative of single emitters;⁹⁰ it was further corroborated by mixing two colors of QDs and observing that most endosomes emitted only one color, which would be highly unlikely if each endosome contained many NGF–QD copies.

Seisenberger et al.⁹¹ observed the infection pathway of viruses singly labeled with Cy5 dyes in living HeLa cells, tracking the viruses as they interacted with the membrane, as they were endocytosed, and as motors directed them inside the cells. The SMS study revealed that the virus infected the cells in much less time than previously observed using bulk experiments, providing insight into the mechanisms that viruses employ to infect cells.

Because the density of macromolecules and cytoskeletal structures is much higher in cells than in the buffers used for in vitro assays, observing how biomolecular motors perform in the typical conditions inside living cells is of particular interest. Cai et al.⁹² studied single kinesin motors in COS mammalian cells, and correlated intensity fluctuations with physiological conditions. They measured the average speed and run length that individual motors, extracted from single-molecule traces. Pierobon et al.⁹³ tracked single myosin motors labeled with QDs in living HeLa cells, measuring even slightly higher velocities than in vitro.^{76, 93} Because these parameters agree with bulk and in vitro assays, the researchers concluded that the molecular crowding within a living cell does not significantly hinder the transport speeds of those motor proteins.

Gene Expression

The Xie group has applied SMS to study gene expression in living *E. coli* bacteria cells,^{36, 94} summarized in a recent review.⁹⁵ These studies explored the stochastic nature of gene expression and probed the dynamics of transcription. Moreover, by watching individual expression events in dividing cells, they were able to follow how events unfurl generations later (see Figure 4).

In order to explore the full dynamics of the system, the researchers probed multiple time scales of protein motion (similar to the approach taken by the Moerner team³⁵ described above). Static emitters were possible to detect above the autofluorescence of cells, but single proteins diffusing in the cytosol moved too quickly to be captured, blurring into background at even at the fastest readout speeds of the CCD cameras. To image these fast-moving emitters, Xie et al. cleverly borrowed a concept from strobe photography: during a 100-ms integration time, a bright 10-ms flash from the laser excited the sample; because the diffusing proteins did not move more than a couple pixels during the laser flash, they appeared as spot instead of a blur in the image. Xie et al. also used this stroboscopic time-lapse technique to image individual proteins diffusing very quickly on DNA, determining the diffusion coefficient by varying the stroboscopic exposure time from 10–100 ms and measuring the molecule's displacement.³⁶

spFRET

Single-pair FRET (spFRET) has been used in a few studies to measure signaling interactions and protein conformations. Many novel observations would have been not possible without spFRET measurements, because the ensemble FRET value does not reveal the dynamics, stoichiometry, binding order, orientation, or temporal information that is observable using SMS.

For instance, using Cy3 and Cy5 fluorophores as the FRET donor and acceptor labels, Sako et al.⁹⁶ observed epidermal growth factor (EGF) receptor signaling in living A431 mammalian cells. The early events in the signaling process include dimerization and autophosphorylation of the receptor. By tracking single EGFs labeled with Cy3 or Cy5, the researchers were able to use spFRET to detect when two copies of the EGF–receptor complex dimerized. They also imaged a Cy3-labeled antibody that binds only to phosphorylated receptors; because the antibody–Cy3 more often colocalized with EGF–Cy5 receptors that were twice as bright as other receptors, the authors determined that the receptor first dimerizes, then phosphorylation occurs after the dimer forms. They were also able to observe that binding of EGF to a dimer of receptors is much stronger than the binding to a monomer, and that EGFs bind one at a time to the receptor dimer, instead of as a pair.

Other researchers explored more dimensions of the spFRET signal in order to separate the details of EGF binding and receptor dimerization. With a polarizer and a dichroic mirror, S. Webb et al.⁹⁷ split the output of the microscope into four regions of the camera, simultaneously measuring the polarization and FRET signals from single EGFs labeled with Cy3 or Cy5. Live A431 cells were incubated with the labeled EGFs, which were allowed to bind to the receptors in the cell surface. FRET efficiency is a complex parameter that depends not only the proximity but also the orientation between the donor and acceptor molecules; by knowing the orientation of the two chromophores (from the polarization of the emission), the two factors in FRET efficiency can be decoupled. Indeed, the researchers observed some events where changes in the spFRET signal were the outcome of orientation changes and other events that resulted from changes in proximity.

Other signaling events have also been measured using spFRET. Murakoshi et al.⁹⁸ applied the technique to observe the activity of Ras, a G protein that influences various signaling pathways

in the cell. Because the precise transduction mechanism of the Ras signal switch is poorly understood, the ability to detect single Ras activating events with spFRET could be helpful. Cells that were engineered to express a Ras–FP were microinjected with guanosine triphosphate (GTP) labeled with a Bodipy organic fluorophore. The researchers monitored binding of the GTP–Bodipy to Ras–FP using the FRET signal from single pairs, and observed that Ras diffusion was subsequently suppressed. Such immobilization after binding events may reveal a larger complex Ras interacts with during signaling.

Super-Resolution SMS Imaging of Life

Background

The spatial resolution of far-field optical microscopy is determined by the diffraction-limited size of the point-spread function. This limit—recognized by Abbe, Rayleigh, and others—means that photons from multiple emitters closer than about half the wavelength of light used cannot be simultaneously resolved spatially when detected in the far-field. However, emitters can be differentiated by taking into account properties of the photons other than just their locations, such as time and wavelength, making the actual photophysics and photochemistry of the emitter more important.

For instance, early work in low-temperature SMS regularly resolved single emitters spaced much closer than the optical diffraction limit: by taking advantage of narrow absorption linewidths and tunable dye lasers, researchers spectrally separated molecules that were spatially close.^{90, 99-101} At biologically relevant temperatures, where linewidths are broad, color alone is insufficient to differentiate many molecules within a diffraction-limited region, and other parameters are necessary for super-resolution SMS. For instance, if a single molecule moves through a structure, localization of the molecule at each time point yields a superresolution image of the structure (see filaments in Figure 4A upper right).³⁵ Photoswitching offers a more generally applicable temporal control of the fluorescence from single molecules, once again giving researchers a property that could be harnessed for super-resolution imaging.

In 2006, three groups independently reported super-resolution imaging based on photoswitching/photoactivation of single molecules (termed PALM, STORM, and FPALM).¹⁰²⁻¹⁰⁴ Super-resolution images are constructed from rounds of photoactivating sparse subsets of a sample and localizing those single emitters with high precision, building up over time a final image with high spatial resolution. Most of the first efforts in super-resolution SMS imaging used nonbiological samples or cells that had been fixed by polymerizing molecules of the cytoplasm, primarily because each image requires hundreds of camera frames and many tens of seconds to acquire. Recently, however, advances in microscope setups and photoactivatable probes—as well as the careful selection of slowly changing (quasi-static) objects—has allowed several groups to obtain super-resolution images of structures and molecular interactions in living cells.

(Other super-resolution techniques, such as stimulated-emission-depletion and structured-illumination microscopies also take advantage of photophysics of fluorophores, as well as sophisticated optical setups, to measure super-resolution images and are applicable to living cells,^{105, 106} however, because these techniques do not inherently require single-molecule detection, they will not be discussed in this Perspective.)

Super-Resolution SMS in Living Cells

S. Hess et al.¹⁰⁷ imaged at high resolution the membrane protein hemagglutinin in fixed and living fibroblast cells using a photoactivatable FP called PA-GFP (see Figure 5). Hemagglutinin has been proposed to associate with nanometer-scale membrane rafts, and

probing protein distributions at high resolution can shed light on raft content and structure. The images revealed irregular, extended clusters of hemagglutinin, thus undermining models of lipid rafts that predict smooth, rounded boundaries, as defined by fluid–fluid phase segregation. Moreover, this study found that fixed cells had quantitatively different protein distribution, confirming that fixing cells can cause nonbiological artifacts.

The team led by Betzig, H. Hess, and Lippincott-Schwartz studied dynamics in living COS-7 cells by combining super-resolution with single-particle tracking to image high-density trajectories of membrane proteins (Gag and VSVG) labeled with a FP called EosFP.¹⁰⁸ Moreover, because many trajectories can be measured in one cell, a map of mobility was constructed for individual cells: clusters of slowly moving proteins were found among large regions of highly mobile molecules. Shroff et al.¹⁰⁹ also imaged the changes in adhesion complex structures over several minutes in living NIH 3T3 cells labeled with EosFP. By obtaining super-resolution images in a time series, the researchers were able to display how the structures grow and changes as the cell moved (see Figure 5).

The Moerner team imaged super-resolution structures in living bacteria *C. crescentus*.^{54, 87} Bacteria pose a unique challenge for super-resolution fluorescence imaging: because of their tiny size, only a few diffraction-limited spots can fit within the cell before they are unresolvable. Moreover, cytoskeleton structures and protein localization is particularly of interest in *C. crescentus*, in order to help explain the mechanisms of asymmetric cell division. In one study, a Cy3–Cy5 covalent heterodimer was synthesized and the outside of *C. crescentus* cells were coated with the photoswitching molecule.⁵⁴ Super-resolution images of the spindle-like stalk were obtained (see Figure 5). Because the Cy3/Cy5 photoswitching system requires the addition of thiol at high concentration, imaging using those fluorophores inside cells faces serious challenges, thus the first demonstration of the use of this fluorophore pair in a live cell was aimed at a bacterial extracellular stalk.⁵⁴

Therefore, a different approach was taken for imaging the internal cytoskeletal protein MreB in living *C. crescentus* using EYFP,⁸⁷ which the Moerner lab demonstrated was a photoswitch over a decade ago.²⁴ The integration time per CCD frame was chosen carefully so that MreB proteins incorporated in the cytoskeleton were imaged, but unbound monomers moved too fast to be captured. In addition, time-lapse imaging was employed in order fill in some gaps in the cytoskeleton structure (see Figure 5). This approach was possible because MreB proteins treadmill along the polymerized structure,³⁵ as discussed above.

Perspective

While ensemble biochemistry and imaging experiments will always be fundamental to cell biology, SMS has proven itself over the last decade as an invaluable tool for probing heterogeneous populations, dynamics, stoichiometry, trafficking, and structure inside living cells. The future of live-cell SMS is flush with promise, including advances from super-resolution biophysics to controllable emitters, from high-sensitivity detection to fast integration times, from new optical techniques to advances in image processing.

There are limits to what we can learn about biology by studying only isolated cells; therefore, SMS in living systems is progressing toward more complex environments, including cell–cell interactions and whole-organism studies. For instance, researchers have recently begun imaging single molecules within tissues of living vertebrates.¹¹⁰ Moreover, interfacing living cells with tools such as supported lipid bilayers may facilitate imaging cell–cell interactions and signaling pathways in conditions similar to those inside organisms.¹¹¹

Adaptive optics and wavefront engineering, the state-of-the-art in astronomy, are beginning to appear in cell imaging and SMS.^{112, 113} Wavefront correction in real time may be able to

reduce aberrations from cells or media, but will require fast software feedback. In addition, custom shaping of the point-spread function (on the excitation or the detection side) will allow researchers to encode more information, such as axial position, into SMS images.¹¹³ Other advances in bulk biological microscopy, such as light-sheet illumination and nonlinear optics, will be applicable to SMS as the techniques and instrumentations are refined.¹¹⁴

Super-resolution SMS techniques and single-molecule tracking in living cells will require faster, more sensitive cameras. Alternatively, faster confocal scanning techniques (such as the Nipkow spinning disk), if their optical throughput can be increased significantly, could offer video-rate imaging with the capability to reject out-of-focus background.^{115, 116} Super-resolution methods also need multicolor sources that switch between many colors quickly, are easy to use, can be effectively filter, and integrate into a conventional SMS microscope setup. For instance, sets of light-emitting diodes and/or tunable filters used in conjunction with lamps or white-light lasers could serve as multicolor sources.

Live-cell imaging and super-resolution SMS both are limited by probe photophysics and labeling techniques (see Tables 1 and 2). Increasing localization precision and tracking times require probes with much higher photostability; super-resolution of dynamic structures will require photoswitches that cycle many times and emit several thousands of photons each cycle. Advances in SMS of living cells will require new and improved specific labeling methods that are bioorthogonal, fast, effective, and nonperturbing. Moreover, all super-resolution techniques require high-density specific labeling without altering phenotype.

Regardless of these challenges, SMS in living cells has potential to reveal a new and unexplored level of detail in biology and medicine.

Acknowledgments

We have attempted to include most of the published studies from this quickly growing field, and apologize to researchers inevitably omitted from this Perspective. We thank Maxime Dahan and Marija Vrljic for helpful discussions. This work was supported in part by National Institute of General Medical Sciences Grant Number R01GM086196.

References

1. Smith SB, Finzi L, Bustamante C. *Science* 1992;258:1122–1126. [PubMed: 1439819]
2. Svoboda K, Schmidt CF, Schnapp BJ, Block SM. *Nature* 1993;365:721–727. [PubMed: 8413650]
3. Strick TR, Allemand J, Bensimon D, Bensimon A, Croquette V. *Science* 1996;271:1835–1837. [PubMed: 8596951]
4. Florin E, Moy V, Gaub H. *Science* 1994;264:415–417. [PubMed: 8153628]
5. Rotman B. *Proc. Natl. Acad. Sci. U.S.A* 1961;47:1981–1991. [PubMed: 14038788]
6. Morikawa K, Yanagida M. *J. Biochem* 1981;89:693–696. [PubMed: 6165713]
7. Perkins TT, Quake SR, Smith DE, Chu S. *Science* 1994;264:822–826. [PubMed: 8171336]
8. Barak LS, Webb WW. *J. Cell Biol* 1982;95:846–852. [PubMed: 6296157]
9. Mehta AD, Reif M, Spudich JA, Smith DA, Simmons RM. *Science* 1999;283:1689–1695. [PubMed: 10073927]
10. Lakadamyali M, Rust MJ, Babcock HP, Zhuang X. *Proc. Natl. Acad. Sci. U.S.A* 2003;100:9280–9285. [PubMed: 12883000]
11. Rigler, R.; Elson, E.; Elson, E. *Fluorescence Correlation Spectroscopy*, Springer Series in Chemical Physics. Schaefer, FP.; Toennies, JP.; Zinth, W., editors. Vol. 65. Springer; Berlin: 2001.
12. Hess ST, Huang S, Heikal AA, Webb WW. *Biochemistry* 2002;41:697–705. [PubMed: 11790090]
13. Moerner WE, Kador L. *Phys. Rev. Lett* 1989;62:2535–2538. [PubMed: 10040013]
14. Orrit M, Bernard J. *Phys. Rev. Lett* 1990;65:2716–2719. [PubMed: 10042674]

15. Moerner WE. *J. Phys. Chem. B* 2002;106:910–927.
16. Shera EB, Seitzinger NK, Davis LM, Keller RA, Soper SA. *Chem. Phys. Lett* 1990;174:553–557.
17. Eigen M, Rigler R. *Proc. Natl. Acad. Sci. U.S.A* 1994;91:5740–5747. [PubMed: 7517036]
18. Nie S, Chiu DT, Zare RN. *Science* 1994;266:1018–1021. [PubMed: 7973650]
19. Barnes MD, Ng KC, Whitten WB, Ramsey JM. *Anal. Chem* 1993;65:2360–2365.
20. Betzig E, Chichester RJ. *Science* 1993;262:1422–1428. [PubMed: 17736823]
21. Dickson RM, Norris DJ, Tzeng YL, Moerner WE. *Science* 1996;274:966–969. [PubMed: 8875935]
22. Deniz AA, Mukhopadhyay S, Lemke EA. *J. Royal Soc. Interface* 2008;5:15–45.
23. Joo C, Balci H, Ishitsuka Y, Buranachai C, Ha T. *Annu. Rev. Biochem* 2008;77:51–76. [PubMed: 18412538]
24. Dickson RM, Cubitt AB, Tsien RY, Moerner WE. *Nature* 1997;388:355–358. [PubMed: 9237752]
25. Ha T, Enderle T, Ogletree DF, Chemla DS, Selvin PR, Weiss S. *Proc. Natl. Acad. Sci. U.S.A* 1996;93:6264–6268. [PubMed: 8692803]
26. Schmidt T, Schutz GJ, Baumgartner W, Gruber HJ, Schindler H. *Proc. Natl. Acad. Sci. U.S.A* 1996;93:2926–2929. [PubMed: 8610144]
27. Funatsu T, Harada Y, Tokunaga M, Saito K, Yanagida T. *Nature* 1995;374:555–559. [PubMed: 7700383]
28. Sase I, Miyata H, Corrie JE, Craik JS, Kinoshita K Jr. *Biophys. J* 1995;69:323–328. [PubMed: 8527645]
29. Vale RD, Funatsu T, Pierce DW, Romberg L, Harada Y, Yanagida T. *Nature* 1996;380:451–453. [PubMed: 8602245]
30. Sosa H, Peterman EJG, Moerner WE, Goldstein LSB. *Nat. Struct. Biol* 2001;8:540–544. [PubMed: 11373624]
31. Prescher JA, Bertozzi CR. *Nat. Chem. Biol* 2005;1:13–21. [PubMed: 16407987]
32. Chen I, Ting A. *Curr. Opin. Biotech* 2005;16:35–40. [PubMed: 15722013]
33. Adams SR, Campbell RE, Gross LA, Martin BR, Walkup GK, Yao Y, Llopis J, Tsien RY. *J. Am. Chem. Soc* 2002;124:6063–6076. [PubMed: 12022841]
34. Lord SJ, Conley NR, Lee HD, Nishimura SY, Pomerantz AK, Willets KA, Lu Z, Wang H, Liu N, Samuel R, Weber R, Semyonov AN, He M, Twieg RJ, Moerner WE. *ChemPhysChem* 2009;10:55–65. [PubMed: 19025732]
35. Kim SY, Gitai Z, Kinkhabwala A, Shapiro L, Moerner WE. *Proc. Nat. Acad. Sci. U.S.A* 2006;103:10929–10934.
36. Elf J, Li GW, Xie XS. *Science* 2007;316:1191–1194. [PubMed: 17525339]
37. Giepmans BNG, Adams SR, Ellisman MH, Tsien RY. *Science* 2006;312:217–224. [PubMed: 16614209]
38. Chalfie M. *Angew. Chem., Int. Ed* 2009;48:5603–5611.
39. Harms GS, Cognet L, Lommerse PHM, Blab GA, Schmidt T. *Biophys. J* 2001;80:2396–2408. [PubMed: 11325739]
40. Douglass AD, Vale RD. *Methods Cell Biol* 2008;85:113–125. [PubMed: 18155461]
41. Shaner NC, Steinbach PA, Tsien RY. *Nat. Methods* 2005;2:905–909. [PubMed: 16299475]
42. Peterman EJG, Brasselet S, Moerner WE. *J. Phys. Chem. A* 1999;103:10553–10560.
43. Schmidt T, Kubitscheck U, Rohler D, Nienhaus U. *Single Mol* 2002;3:327.
44. Soper SA, Nutter HL, Keller RA, Davis LM, Shera EB. *Photochem. Photobiol* 1993;57:972–977.
45. Margineanu A, Hofkens J, Cotlet M, Habuchi S, Stefan A, Qu J, Kohl C, Mullen K, Vercammen J, Engelborghs Y, Gensch T, De Schryver FC. *J. Phys. Chem. B* 2004;108:12242–12251.
46. Bruchez MJ, Moronne M, Gin P, Weiss S, Alivisatos AP. *Science* 1998;281:2013–2016. [PubMed: 9748157]
47. Resch-Genger U, Grabolle M, Cavaliere-Jaricot S, Nitschke R, Nann T. *Nat. Methods* 2008;5:763–775. [PubMed: 18756197]
48. Richards CI, Choi S, Hsiang J, Antoku Y, Vosch T, Bongiorno A, Tzeng Y, Dickson RM. *J. Am. Chem. Soc* 2008;130:5038–5039. [PubMed: 18345630]

49. Wu S, Han G, Milliron DJ, Aloni S, Altoe V, Talapin DV, Cohen BE, Schuck PJ. *Proc. Nat. Acad. Sci. U.S.A* 2009;106:10917–10921.
50. Lukyanov KA, Chudakov DM, Lukyanov S, Verkhusha VV. *Nat. Rev. Mol. Cell Biol* 2005;6:885–891. [PubMed: 16167053]
51. Lippincott-Schwartz J, Patterson GH. *Methods Cell Biol* 2008;85:45–61. [PubMed: 18155458]
52. Heilemann M, Margeat E, Kasper R, Sauer M, Tinnefeld P. *J. Am. Chem. Soc* 2005;127:3801–3806. [PubMed: 15771514]
53. Bates M, Blosser TR, Zhuang X. *Phys. Rev. Lett* 2005;94:108101-1–108101-4. [PubMed: 15783528]
54. Conley NR, Biteen JS, Moerner WE. *J. Phys. Chem. B* 2008;112:11878–11880. [PubMed: 18754575]
55. Lord SJ, Conley NR, Lee HD, Samuel R, Liu N, Twieg RJ, Moerner WE. *J. Am. Chem. Soc* 2008;130:9204–9205. [PubMed: 18572940]
56. Fölling J, Belov V, Kunetsky R, Medda R, Schönle A, Egner A, Eggeling C, Bossi M, Hell SW. *Angew. Chem. Int. Ed* 2007;46:6266–6270.
57. Marriott G, Mao S, Sakata T, Ran J, Jackson DK, Petchprayoon C, Gomez TJ, Warp E, Tulyathan O, Aaron HL, Isacoff EY, Yan Y. *Proc. Nat. Acad. Sci. U.S.A* 2008;105:17789–17794.
58. Han G, Mokari T, Ajo-Franklin C, Cohen BE. *J. Am. Chem. Soc* 2008;130:15811–15813. [PubMed: 18983148]
59. Tian Z, Wu W, Wan W, Li ADQ. *J. Am. Chem. Soc* 2009;131:4245–4252. [PubMed: 19275146]
60. Fernandez-Suarez M, Ting AY. *Nat. Rev. Mol. Cell Biol* 2008;9:929–943. [PubMed: 19002208]
61. Park H, Hanson GT, Duff SR, Selvin PR. *J. Microsc* 2004;216:199–205. [PubMed: 15566490]
62. O'Hare HM, Johnsson K, Gautier A. *Curr. Opin. Struct. Biol* 2007;17:488–494. [PubMed: 17851069]
63. Moerner WE, Fromm DP. *Rev. Sci. Instrum* 2003;74:3597–3619.
64. Michalet X, Siegmund OHW, Vallergera JV, Jelinsky P, Millaud JE, Weiss S. *J. Mod. Opt* 2007;54:239. [PubMed: 20157633]
65. Moerner WE. *Trends Anal. Chem* 2003;22:544–548.
66. Sako Y, Yanagida T. *Nat. Rev. Mol. Cell Biol* 2003;4:SS1–5. [PubMed: 14587519]
67. Vrljic M, Nishimura SY, Moerner WE. *Methods Mol. Biol* 2007;398:193–219. [PubMed: 18214382]
68. Wieser S, Schütz GJ. *Methods* 2008;46:131–140. [PubMed: 18634880]
69. Kusumi A, Nakada C, Ritchie K, Murase K, Suzuki K, Murakoshi H, Kasai RS, Kondo J, Fujiwara T. *Annu. Rev. Biophys. Biomol. Struct* 2005;34:351–378. [PubMed: 15869394]
70. Kusumi A, Sako Y. *Curr. Opin. Cell Biol* 1996;8:566–574. [PubMed: 8791449]
71. Vrljic M, Nishimura SY, Brasselet S, Moerner WE, McConnell HM. *Biophys. J* 2002;83:2681–2692. [PubMed: 12414700]
72. Nishimura SY, Vrljic M, Klein LO, McConnell HM, Moerner WE. *Biophys. J* 2006;90:927–938. [PubMed: 16272447]
73. Nishimura SY, Lord SJ, Klein LO, Willets KA, He M, Lu Z, Twieg RJ, Moerner WE. *J. Phys. Chem. B* 2006;110:8151–8157. [PubMed: 16610918]
74. Umemura YM, Vrljic M, Nishimura SY, Fujiwara TK, Suzuki KGN, Kusumi A. *Biophys. J* 2008;95:435–450. [PubMed: 18339737]
75. Lee HD, Dubikovskaya EA, Hwang H, Semyonov AN, Wang H, Jones LR, Twieg RJ, Moerner WE, Wender PA. *J. Am. Chem. Soc* 2008;130:9364–9370. [PubMed: 18578528]
76. Dahan M, Levi S, Luccardini C, Rostaing P, Riveau B, Triller A. *Science* 2003;302:442–445. [PubMed: 14564008]
77. Harms GS, Cagnet L, Lommerse PHM, Blab GA, Kahr H, Gamsjaeger R, Spaink HP, Soldatov NM, Romanin C, Schmidt T. *Biophys. J* 2001;81:2639–2646. [PubMed: 11606277]
78. Schütz GJ, Pastushenko VP, Gruber HJ, Knaus H, Pragl B, Schindler H. *Single Mol* 2000;1:25–31.
79. Ueda M, Sako Y, Tanaka T, Devreotes P, Yanagida T. *Science* 2001;294:864–867. [PubMed: 11679673]
80. Ulbrich MH, Isacoff EY. *Nat. Methods* 2007;4:319–321. [PubMed: 17369835]
81. Haggie PM, Verkman AS. *J. Biol. Chem* 2008;283:23510–23513. [PubMed: 18617526]
82. Yang W, Gelles J, Musser SM. *Proc. Nat. Acad. Sci. U.S.A* 2004;101:12887–12892.

83. Kubitscheck U, Grunwald D, Hoekstra A, Rohleder D, Kues T, Siebrasse JP, Peters R. *J. Cell Biol* 2005;168:233–243. [PubMed: 15657394]
84. Knemeyer J, Herten D, Sauer M. *Anal. Chem* 2003;75:2147–2153. [PubMed: 12720354]
85. Deich J, Judd EM, McAdams HH, Moerner WE. *Proc. Nat. Acad. Sci. U.S.A* 2004;101:15921–15926.
86. Bowman GR, Comolli LR, Zhu J, Eckart M, Koenig M, Downing KH, Moerner WE, Earnest T, Shapiro L. *Cell* 2008;134:945–955. [PubMed: 18805088]
87. Biteen JS, Thompson MA, Tselentis NK, Bowman GR, Shapiro L, Moerner WE. *Nat. Methods* 2008;5:947–949. [PubMed: 18794860]
88. Niu L, Yu P. *Biophys. J* 2008;95:2009–2016. [PubMed: 18390602]
89. Cui B, Wu C, Chen L, Ramirez A, Bearer EL, Li W, Mobley WC, Chu S. *Proc. Nat. Acad. Sci. U.S.A* 2007;104:13666–13671.
90. Ambrose WP, Basché T, Moerner WE. *J. Chem. Phys* 1991;95:7150–7163.
91. Seisenberger G, Ried MU, Endress T, Buning H, Hallek M, Braeuchle C. *Science* 2001;294:1929–1932. [PubMed: 11729319]
92. Cai D, Verhey KJ, Meyhöfer E. *Biophys. J* 2007;92:4137–4144. [PubMed: 17400704]
93. Pierobon P, Achouri S, Courty S, Dunn AR, Spudich JA, Dahan M, Cappello G. *Biophys. J* 2009;96:4268–4275. [PubMed: 19450497]
94. Yu J, Xiao J, Ren X, Lao K, Xie XS. *Science* 2006;311:1600–1603. [PubMed: 16543458]
95. Xie XS, Choi PJ, Li GW, Lee NK, Lia G. *Annu. Rev. Biophys* 2008;37:417–444. [PubMed: 18573089]
96. Sako Y, Minoghchi S, Yanagida T. *Nat. Cell Biol* 2000;2:168–172. [PubMed: 10707088]
97. Webb SED, Needham SR, Roberts SK, Martin-Fernandez ML. *Opt. Lett* 2006;31:2157–2159. [PubMed: 16794711]
98. Murakoshi H, Iino R, Kobayashi T, Fujiwara T, Ohshima C, Yoshimura A, Kusumi A. *Proc. Nat. Acad. Sci. U.S.A* 2004;101:7317–7322.
99. Ambrose WP, Moerner WE. *Nature* 1991;349:225–227.
100. Betzig E. *Opt. Lett* 1995;20:237–239. [PubMed: 19859146]
101. van Oijen AM, Köhler J, Schmidt J, Müller M, Brakenhoff GJ. *Chem. Phys. Lett* 1998;292:183–187.
102. Betzig E, Patterson GH, Sougrat R, Lindwasser OW, Olenych S, Bonifacino JS, Davidson MW, Lippincott-Schwartz J, Hess HF. *Science* 2006;313:1642–1645. [PubMed: 16902090]
103. Rust MJ, Bates M, Zhuang X. *Nat. Methods* 2006;3:793–795. [PubMed: 16896339]
104. Hess ST, Girirajan TPK, Mason MD. *Biophys. J* 2006;91:4258–4272. [PubMed: 16980368]
105. Westphal V, Rizzoli SO, Lauterbach MA, Kamin D, Jahn R, Hell SW. *Science* 2008;320:246–249. [PubMed: 18292304]
106. Kner P, Chhun BB, Griffis ER, Winoto L, Gustafsson MGL. *Nat. Methods* 2009;6:339–342. [PubMed: 19404253]
107. Hess ST, Gould TJ, Gudheti MV, Maas SA, Mills KD, Zimmerberg J. *Proc. Natl Acad. Sci. U.S.A* 2007;104:17370–17375. [PubMed: 17959773]
108. Manley S, Gillette JM, Patterson GH, Shroff H, Hess HF, Betzig E, Lippincott-Schwartz J. *Nat. Methods* 2008;5:155–157. [PubMed: 18193054]
109. Shroff H, Galbraith CG, Galbraith JA, Betzig E. *Nat. Methods* 2008;5:417–423. [PubMed: 18408726]
110. Schaaf MJM, Koopmans WJA, Meckel T, van Noort J, Snaar-Jagalska B, Schmidt TS, Spaink HP. *Biophys. J* 2009;97:1206–1214. [PubMed: 19686669]
111. Hartman NC, Nye JA, Groves JT. *Proc. Natl Acad. Sci. U.S.A* 2009;106:12729–12734. [PubMed: 19622735]
112. Lutz C, Otis TS, DeSars V, Charpak S, DiGregorio DA, Emiliani V. *Nat. Methods* 2008;5:821–827. [PubMed: 19160517]
113. Pavani SRP, Thompson MA, Biteen JS, Lord SJ, Liu N, Twieg RJ, Piestun R, Moerner WE. *Proc. Nat. Acad. Sci. U.S.A* 2009;106:2995–2999.

114. Wilt BA, Burns LD, Wei Ho ET, Ghosh KK, Mukamel EA, Schnitzer MJ. *Annu. Rev. Neurosci* 2009;32:435–506. [PubMed: 19555292]
115. Tadakuma H, Yamaguchi J, Ishihama Y, Funatsu T. *Biochem. Biophys. Res. Commun* 2001;287:323–327. [PubMed: 11554728]
116. Botcherby EJ, Booth MJ, Juskaitis R, Wilson T. *Opt. Express* 2008;16:21843–21848. [PubMed: 19104617]
117. Howard J, Hudspeth AJ, Vale RD. *Nature* 1989;342:154–158. [PubMed: 2530455]
118. Pierce DW, Hom-Booher N, Vale RD. *Nature* 1997;388:338–338. [PubMed: 9237750]
119. Dickson RM, Norris DJ, Moerner WE. *Phys. Rev. Lett* 1998;81:5322–5325.
120. Yildiz A, Forkey JN, McKinner SA, Ha T, Goldman YE, Selvin PR. *Science* 2003;300:2061–2065. [PubMed: 12791999]
121. Churchman LS, Oekten Z, Rock RS, Dawson JF, Spudich JA. *Proc. Nat. Acad. Sci. U.S.A* 2005;102:1419–1423.
122. Tani T, Miyamoto Y, Fujimori KE, Taguchi T, Yanagida T, Sako Y, Harada Y. *J. Neurosci* 2005;25:2181–2191. [PubMed: 15745944]
123. Courty S, Luccardini C, Bellaiche Y, Cappello G, Dahan M. *Nano Lett* 2006;6:1491–1495. [PubMed: 16834436]

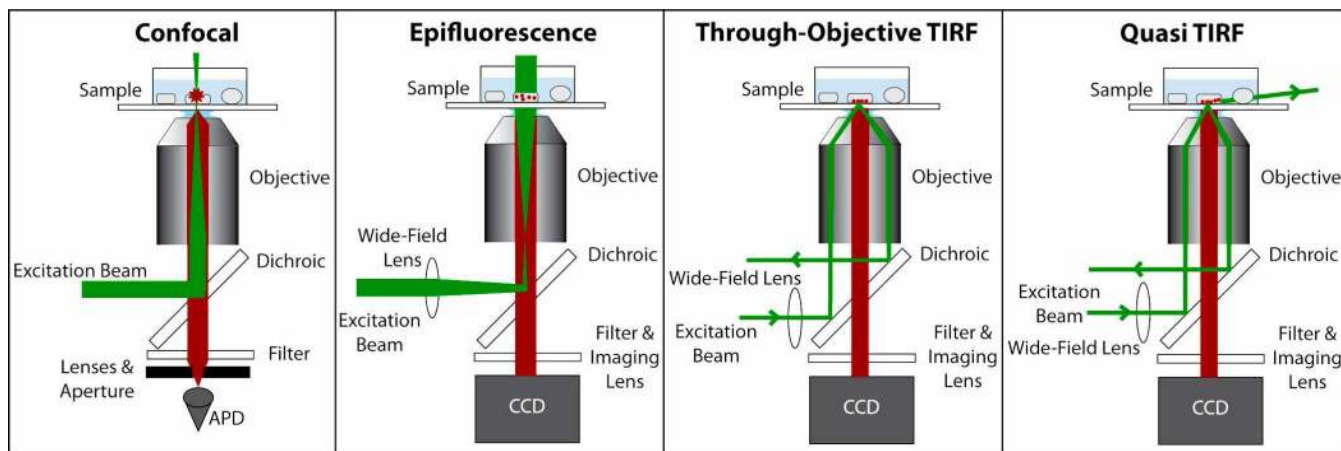


Figure 1.
Generalized microscope configurations for single-molecule imaging in living cells.

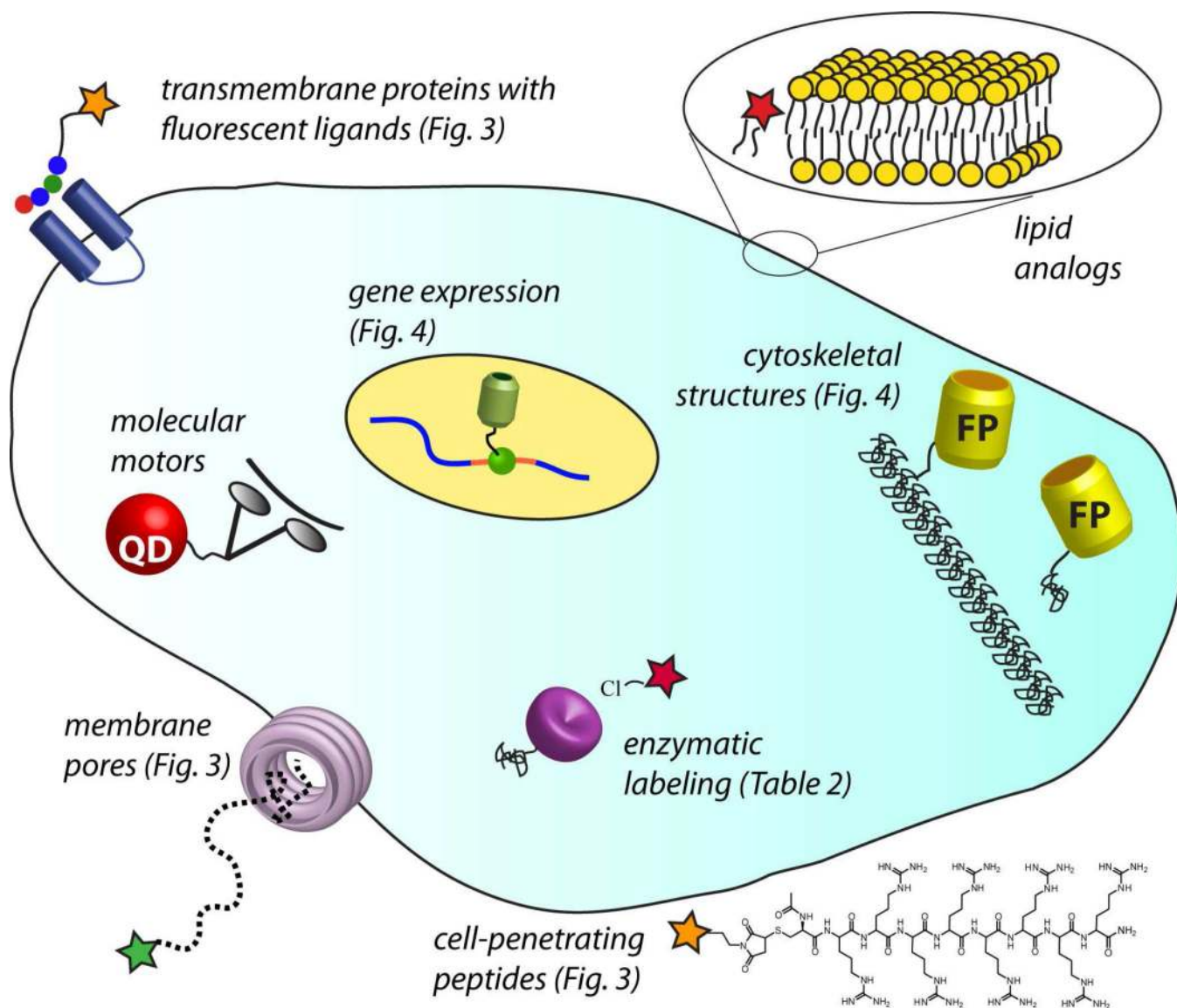


Figure 2.
Some general approaches to SMS in live cells.

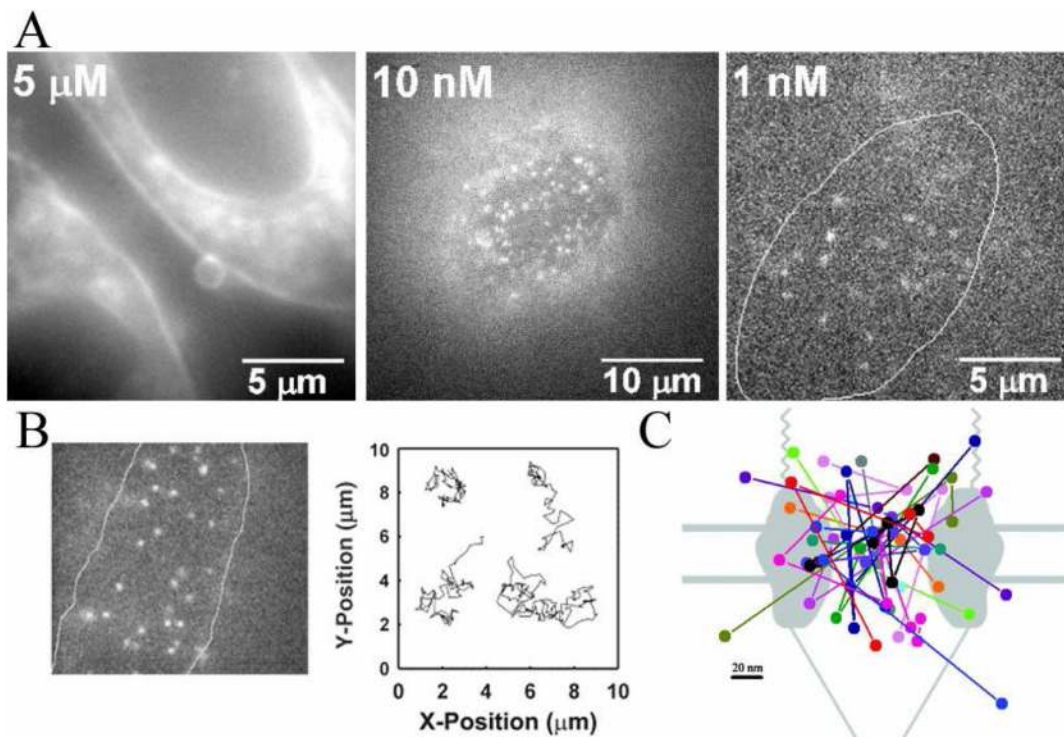


Figure 3.

Single molecules in cell membranes. (A) Cell-penetrating peptides labeled with a DCDHF organic fluorophore in the plasma membrane of mammalian cells. At low enough concentrations of labeled peptides, single molecules can be visible as they interact with the top surface of the cell; at higher concentrations, it is obvious that the fluorophores are bright while in the membrane and in particular regions of the cytosol. These images were taken in epifluorescence mode, required in order to probe the top surface of the cell in widefield. From reference ⁷⁵. (B) (*left*) A snapshot of single transmembrane proteins on the surface of a living mammalian cell. Antigen ligand peptides were labeled with Cy5 and allowed to bind strongly to the transmembrane proteins. This epifluorescence image represents 12×12 μm at the sample plane, with an integration time of 100 ms. (*right*) Examples of single-molecule trajectories. From references ^{65, 71}. (C) Several successive trajectories of single copies of a fluorescently labeled substrate interacting with a nuclear pore complex in living cells. These measurements used a widefield configuration but added a 400-μm pinhole to restrict the imaging area and reduce background fluorescence. From reference ⁸² (© 2004 The National Academy of Sciences of the USA).

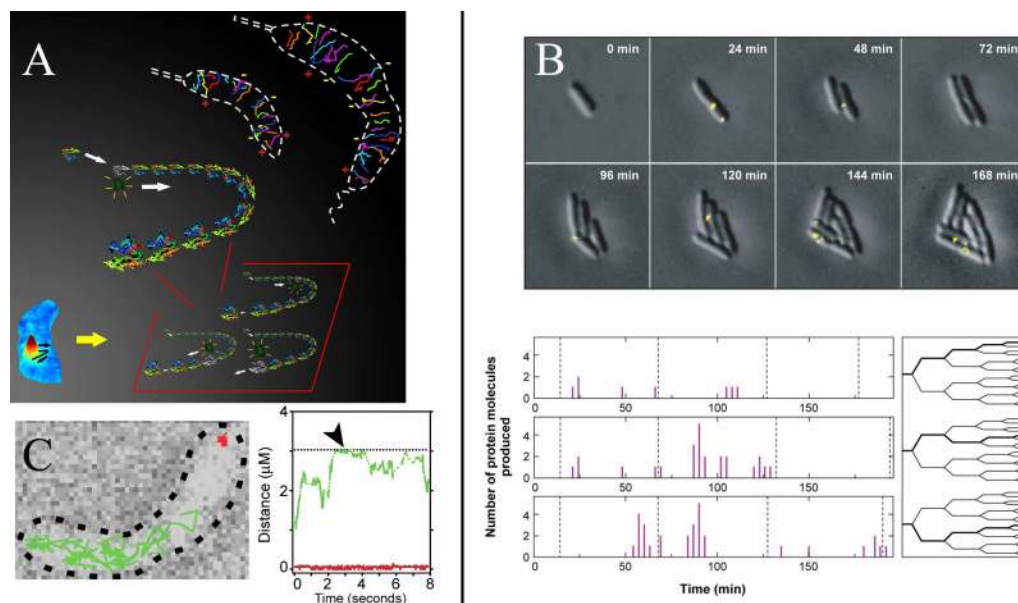


Figure 4.

Single molecules in bacteria. (A) FP-labeled MreB, an actin homolog, shows treadmilling through short MreB filaments in a living *C. crescentus* cell. Directional motion of MreB–FP was measured by imaging single copies of MreB–FP. Single molecules trace out the filaments and the cytoskeletal structure, exhibiting direction and zig-zag motions (bottom left). The diagrams in the center depict the mechanism of treadmilling and motion of MreB monomers in filaments. The cells in the upper right represent several trajectories of the movements of single MreB–FP, tracing out filaments. The + (toward the so-called “stalked” pole of the cell) and – (toward the “swarmer” pole) signs indicate the direction of the movement. See reference ³⁵. (B) Gene expression visualized on the individual-cell and single-molecule scale. (*top*) Time-lapse movie of fluorescence images (yellow) overlaid with simultaneous white-light images (gray) show *E. coli* cells expressing single FP-labeled proteins (sporadic bursts of yellow). (*bottom*) Time traces of the expression of proteins along three particular cell lineages extracted from time-lapse fluorescence movies. The vertical axis is the number of protein molecules newly synthesized during the last three minutes. The dotted lines mark the cell division times. The time traces show that protein production occurs in random bursts, within which variable numbers of protein molecules are generated. From reference ⁹⁴. (C) Single PopZ–FP molecules in a living *C. crescentus* cell. (*left*) Time-lapse visualization of two molecules in a cell, with colored lines tracking the distance moved between frames. One molecule (red) remains localized to the pole, and the other (green) has increased mobility. The tracks are overlaid on a transmitted light image of the cell, outlined in black. (*right*) A representation of the data from the experiment, showing the distance of the molecules from one pole as a function of time. The black horizontal dotted line marks the opposite pole; the red and green lines follow the stationary and mobilized molecules, respectively. From reference ⁸⁶.

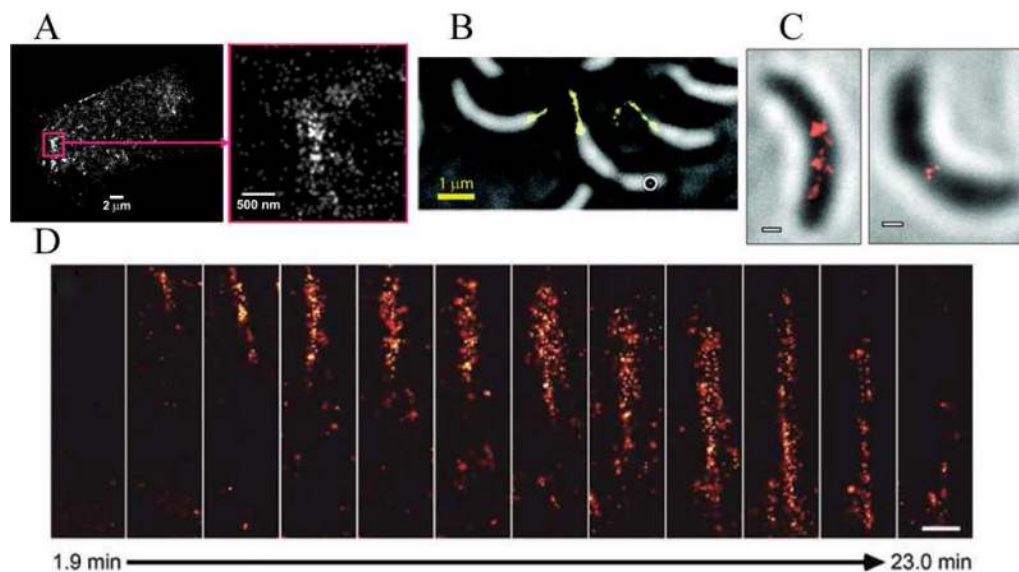


Figure 5.

First live-cell super-resolution SMS experiments. (A) Clusters of hemagglutinin in the membrane of a living fibroblast cell. The right frame is a zoomed-in portion of the left image. The jagged border of the cluster helped eliminate some models for membrane rafts. From reference ¹⁰⁷ (© 2007 The National Academy of Sciences of the USA). (B) Super-resolution fluorescence image of *C. crescentus* stalks labeled with a Cy3–Cy5 covalent pair (yellow) superimposed on a white-light image of the cells (gray). From reference ⁵⁴. (C) Time-lapse super-resolution images of FP-labeled MreB in living *C. crescentus* cell. (*left*) Quasi-helical structure of MreB in a stalked cell. (*right*) Midplane ring of MreB in a predivisional cell. Scale bars, 300 nm. From reference ⁸⁷. (D) Imaging dynamics of an adhesion complex. Time-lapse super-resolution images in a small region of a live NIH 3T3 cell expressing a photoswitchable FP fused to paxillin. Multiple super-resolution images were obtained over an extended period to observe the morphologies and dynamics of the signal-transduction protein paxillin as the adhesion complex formed and elongated at the edge of the cells. These snapshots are high magnification of a single adhesion complex, revealing molecular organization during the elongation process. Scale bar, 500 nm. From reference ¹⁰⁹.

Table 1

Selected Single-Molecule Experiments with Relevance to Living Cells.

Year	Milestone (Living Cells in Bold)	Researchers	References
1961	catalytic activity from one enzyme measured (by observing the build-up of fluorescence from a fluorogenic substrate)	Rotman	5
1981	single strands of DNA visualized (labeled with many fluorophores)	Yanagida, Chu	6, 7
1982	diffusion of single membrane-bound receptor molecules measured (labeled with many fluorophores)	W. Webb	8
1989, 1990	first optical detection of single chromophore in condensed matter (cryogenic)	Moerner, Orrit	13-15
	action from single molecular motors recorded by observing motion of filaments (e.g. sliding assays)	Vale, Yanagida, Spudich	117
1990	room-temperature detection of single molecules from burst analysis in solution	Keller, Rigler, Zare	16-18
1991	first imaging of a single molecule (cryogenic)	Moerner	15, 99
1992	elastic measurements of single strands of DNA using magnetic tweezers	Bustamante, Croquette, Bensimon	1, 3
1993	room-temperature SMS using near-field tips	Betzig	20
	room-temperature SMS in microdroplets	Ramsey	19
	force studies of single macromolecules using optical tweezers or cantilevers	Block, Gaub	2, 4
1995	single motor molecules imaged	Yanagida, Kinoshita, Vale	27-29
1996	3D nanoscale tracking of single emitters, using TIRF evanescent field	Moerner	21
	first single-pair FRET measurements	Weiss, Ha	25
	diffusion of single emitters recorded in a phospholipid membrane	Schmidt, Schindler	26
1997	first SMS of fluorescent proteins	Moerner, Tsien, Vale	24, 118
	first room-temperature SMS example of controlled photoswitching, a fluorescent protein	Moerner, Tsien	24
1998	3D orientations of single molecules measured from dipole emission pattern (room-temperature)	Moerner	119

Year	Milestone (Living Cells in Bold)	Researchers	References
	3D super-resolution by spectral selection of single molecules (cryogenic)	Betzig, van Oijen, Schmidt, Moerner	90, 99-101
2000	spFRET measured in living cells	Yanagida, Kusumi, S. Webb	96-98
	3D tracking of single fluorophores in living cells	Schütz, Schindler	78
	transmembrane ion channels tracked	Schmidt, Schütz, Schindler	77, 78
2001	nucleotide-dependent orientations of single kinesin motors measured	Moerner, Goldstein	30
	binding kinetics to chemotactic receptors in the membrane observed	Yanagida	79
	infection pathway of singly-labeled viruses observed	Brauchle	91
2002	SMS in membranes	Moerner, McConnell, Kusumi, Dahan, Triller	67-69, 71-74, 76
2003	single motor proteins tracked with high precision and super-resolution	Selvin, Spudich	120, 121
2004	protein localization and movement in living bacteria cells using FP labels	Moerner, Shapiro, McAdams	35, 85-87
	molecules tracked through nuclear pore complexes	Musser	82
2005	nerve growth factor tracked in living neurons	Tani, Yanagida, Chu, Mobley, Cui	89, 122
2006	high-precision tracing of filaments in living bacteria	Moerner, Shapiro	35
	super-resolution SMS techniques PALM, STORM, and FPALM introduced	Betzig, H. Hess, Lippincott-Schwartz, Zhuang, S. Hess	102-104
	single-molecule gene expression events studied in living bacteria	Xie	36, 94, 95
	singly-labeled molecular motors observed in living cells	Meyhöfer, Dahan, Cappello, Spudich	92, 93, 123
2007	super-resolution SMS images of living cells	Betzig, H. Hess, Lippincott-Schwartz, S. Hess, Moerner	54, 87, 107-109
	SMS used to count the number of subunits in membrane-bound proteins	Isacoff, Verkman	80, 81
2008	interaction of cell-penetrating peptides with membrane observed	Moerner, Wender	75
	single monomers of the cytoskeletal protein photoactivated and tracked	Yu	88
2009	SMS in living vertebrates	Schmidt, Schaaf	110

Table 2

Fluorophores for SMS in Living Cells.

Fluorophore	Advantage	Disadvantage	Photoactivatable?	References
FPs	genetically expressed	less photostable (only ~100,000 photons emitted per molecule)		37, 39, 41, 43
GFP		too blue (<500 nm excitation required)	no	
EYFP	>500 nm excitation		yes	24
Organic Fluorophores	small, tunable, photostable (millions of photons emitted per molecule)	challenging labeling		43
FlAsH/ReAsH	specific labeling	less photostable	no	33
rhodamines	photostable, bright		yes	44, 56
cyanine dyes	photostable, bright		yes	53
DCDHF _s	photostable, red, environmental sensing, enter cells		yes	34, 55
QDs and Nanoparticles	photostable (tens of millions of photons or more emitted per particle)	large, cell entry, challenging labeling, blinky		46, 47
caged QDs	photoactivatable		yes	58
silver nanoclusters	high cross-section		no	48
photoswitching polymer nanoparticles	photoswitchable		yes	59
upconverting nanoparticles	very photostable, pumped in NIR		no	49

Table 3

Labeling Approaches for SMS in Living Cells.

Labeling Technique	Examples	Applicable Systems	Developments Needed	References
Genetic Expression of FPs	EYFP	live cells	increased photostability	37, 39, 41, 43
Enzymatic Tags	Halo, SNAP, BirA, Sfp-CoA	live cells	better washing, smaller fusion	32, 62
Genetic Peptide Tags	FIAsh	live cells, typically bulk imaging	reduce off-target labeling, strengthen binding	32, 33, 37, 62
Antibodies	biotin/streptavidin	fixed cells, surfaces of live cells	stronger binding, smaller size, expanded applications for live cells	32, 37, 62
Bioorthogonal Rxns	click	typically surfaces of live cells	simple expression of reactive tags	31
Nonspecific Labeling	maleimide, NHS ester	in vitro labeling of biomolecules	better routes to introduce exogenous molecules into cells	